NANO LETTERS

Letter

pubs.acs.org/NanoLett

Ultrafast Phase Transition via Catastrophic Phonon Collapse Driven by Plasmonic Hot-Electron Injection

Kannatassen Appavoo,*[,†,‡] Bin Wang,[§] Nathaniel F. Brady,[∥] Minah Seo,[⊥] Joyeeta Nag,[§] Rohit P. Prasankumar,[⊥] David J. Hilton,[∥] Sokrates T. Pantelides,[§,¶,□] and Richard F. Haglund, Jr.*[,†,§]

[†]Interdisciplinary Materials Science, Vanderbilt University, Nashville, Tennessee 37235-0106, United States

[‡]Center for Functional Nanomaterials, Brookhaven National Laboratory, Upton, New York 11973, United States

[§]Department of Physics and Astronomy, Vanderbilt University, Nashville, Tennessee 37235-1807, United States

[∥]Department of Physics, The University of Alabama, Birmingham, Alabama 35294, United States

[⊥]Center for Integrated Nanotechnologies, Los Alamos National Laboratory, Los Alamos, New Mexico 87545, United States

[¶]Materials Science and Technology Division, Oak Ridge National Laboratory, Oak Ridge, Tennessee 37831, United States

[□]Department of Electrical Engineering and Computer Science, Vanderbilt University, Nashville, Tennessee 37235, United States

Supporting Information

ABSTRACT: Ultrafast photoinduced phase transitions could revolutionize data-storage and telecommunications technologies by modulating signals in integrated nanocircuits at terahertz speeds. In quantum phase-changing materials (PCMs), microscopic charge, lattice, and orbital degrees of freedom interact cooperatively to modify macroscopic electrical and optical properties. Although these interactions are well documented for bulk single crystals and thin films, little is known about the ultrafast dynamics of nanostructured PCMs when interfaced to another class of materials as in this case to active plasmonic elements. Here, we demonstrate how a mesh of gold nanoparticles, acting as a plasmonic photocathode, induces an ultrafast phase transition in nanostructured vanadium dioxide (VO_2) when illuminated by a spectrally resonant femtosecond laser pulse. Hot electrons created by optical excitation of the surface-plasmon resonance in the gold nanomesh are injected ballistically across the Au/VO_2 interface to induce a subpicosecond phase transformation in VO_2. Density functional calculations show that a critical density of injected electrons leads to a catastrophic collapse of the 6 THz phonon mode, which has been linked in different experiments to VO_2 phase transition. The demonstration of subpicosecond phase transformations that are triggered by optically induced electron injection opens the possibility of designing hybrid nanostructures with unique nonequilibrium properties as a critical step for all-optical nanophotonic devices with optimizable switching thresholds.

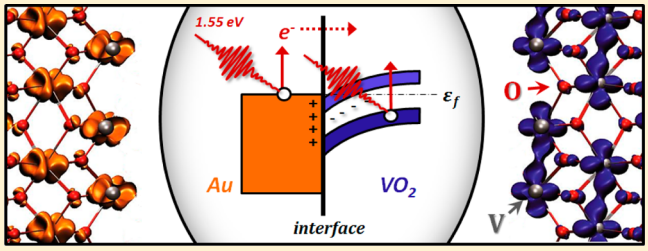

KEYWORDS: *ultrafast phase-transition, plasmonic, electron injection, vanadium dioxide, phonon mode*

Phase transitions in quantum materials can provide functionality in nanophotonic devices[1,2] because the interplay among microscopic charge, lattice, and orbital[3,4] degrees of freedom conspires to generate tunable macroscopic quantum phenomena such as multiferroicity,[5] insulator-to-metal transitions,[6] and colossal magnetoresistance.[7] Ultrafast optical excitation of phase-changing materials (PCMs) provides the ultimate noncontact control over these properties by creating transient states of matter not readily accessible under equilibrium conditions. Recently, phase-transition (PT) events have even been shown to occur on a time scale shorter than a single phonon period, driven by a rapid modification in the lattice potential-energy surface.[8,9] These observations suggest that the PT can perhaps be triggered on even faster time scales by ultrafast perturbation of the lattice potential, possibly even revealing the ultimate mechanism for the optically induced PT. Moreover, in a recent study by Hada et al.[10] the PT in vanadium dioxide (VO_2) was triggered at time scales of tens of picoseconds, induced by electrons that were excited in a thick gold electrode by a femtosecond laser and injected into VO_2 by an applied electric field. At these time scales, the excited electrons have already achieved equilibrium with the lattice.

In this Letter, we demonstrate an all-optical method for triggering the PT in VO_2 on a femtosecond time scale by *nonequilibrium* hot electrons. By exploiting the properties of plasmonics, ballistic electrons generated by femtosecond laser excitation of a sparse network of gold nanoparticles are photoinjected into vanadium dioxide (VO_2) nanoislands across the Au/VO_2 interface. The resonant plasmonic excitation of the metallic nanostructures results in a subpicosecond photo-injection process that reduces the switching threshold by at

Received: August 23, 2013
Published: January 31, 2014

   dx.doi.org/10.1021/nl4044828 | *Nano Lett.* 2014, 14, 1127−1133

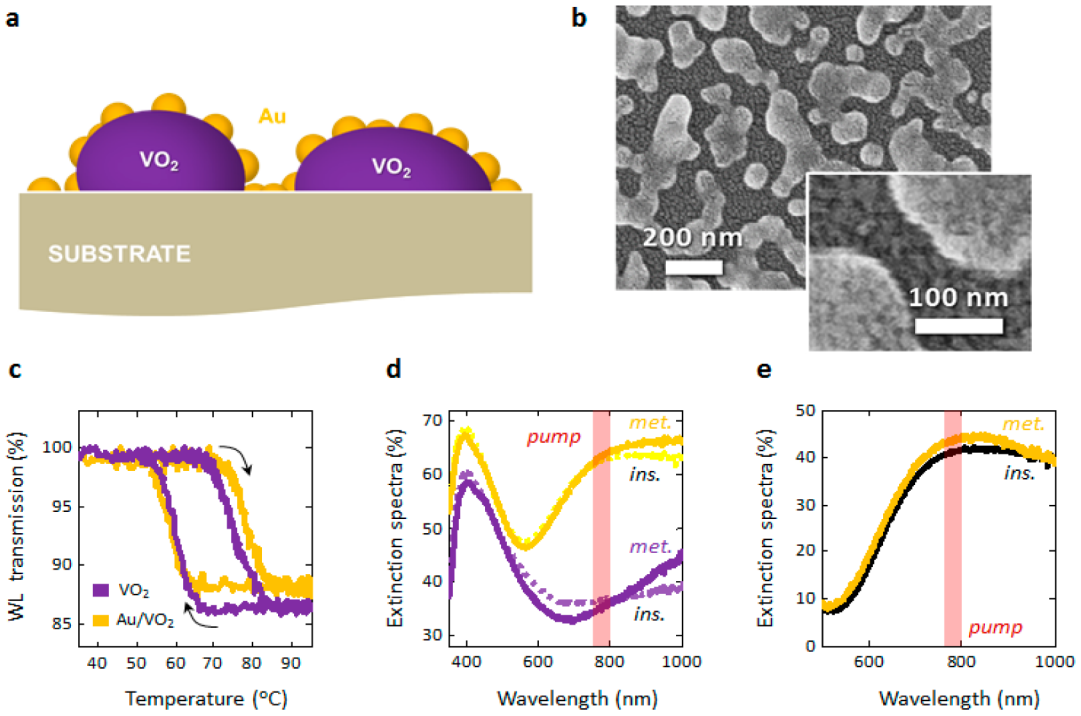

Figure 1. Characterization of hybrid Au/PCM-VO_2 nanomaterial. (a) Schematic of the hybrid nanomaterial with 5 nm thin Au-nanomesh coating the vanadium dioxide nanoislands (40 nm nominal height). (b) Scanning electron micrograph of the hybrid nanomaterial. (c) White-light transmission hysteresis measurement of Au/VO_2 hybrid (yellow) and pristine VO_2 nanoislands (purple) samples when modulated thermally. Note that T_c is ~68 °C in both cases. (d) Extinction spectra of the two samples (purple: pristine VO_2 and yellow: Au/VO_2) when at 25 °C (insulating VO_2) and 100 °C (metallic VO_2). Note the increase in extinction in both cases where the VO_2 switches metallic (darker yellow and darker purple) (e) Differential extinction spectra of panel (d), depicting the plasmonic response of the Au-nanomesh that blue shifts slightly when the VO_2 switches from insulating (black) to metallic (yellow).

least a factor of 5 in the nonequilibrium limit. Furthermore, we demonstrate that the ultrafast response of this hybrid nanostructure is distinctly different from that of the pristine VO_2 material.

Density functional calculations are used to explore possible mechanisms for the observed ultrafast PT triggered by injected electrons. We find that a critical density of injected electrons causes a catastrophic collapse of the A_{1g} phonon mode of the insulating VO_2 lattice, resulting in the observed subpicosecond insulator-to-metal transition. These results therefore illustrate how plasmon damping by hot-electron effects, detrimental in plasmonic circuitry due to linewidth broadening,[11] can actually be harnessed constructively when combined with PT processes. More importantly, when compared to the pristine PCM, the properties of the hybrid nanomaterial remain unaffected in the steady-state thermal equilibrium limit while exhibiting a radically different response in the nonequilibrium regime.

Previous studies of hybrid materials comprising plasmonic and phase-changing components have used the phase transition to trigger modulation of plasmon wavelength[2,12] or used the plasmon resonance or linewidth as a probe of the quantum material.[13−15] Recently, optical devices incorporating vanadium dioxide have also been described.[16,17] In these studies, the VO_2 is deployed in a way that uses the phase transition in thermal equilibrium and on micrometer scale lengths to alter plasmonic response. In contrast to these examples, in the present work, the hybrid nanostructure is itself considered as a reconfigurable, nanoscale design element, in which the active, electronic response of the plasmon is used to induce a dynamic response in the phase-changing material on a nonequilibrium time scale.

To demonstrate this general design strategy, samples of the hybrid nanomaterial are fabricated first by growing VO_2 nanoislands on quartz substrate by a pulsed-laser deposition method:[18] (i) ablation of a vanadium metal target using a KrF excimer laser (λ = 248 nm; 25 ns pulse duration; 3.84 J/cm^2 fluence, 25 Hz repetition rate, 40 nm nominal thickness) in 10 mTorr of O_2 environment; (ii) a subsequent thermal anneal at 450 °C in 250 mTorr of O_2 for 45 min to render the nanoislands stoichiometric and crystalline in the M1 insulating-phase, which exhibits switching behavior, that is, a phase transformation to a metallic phase at 68 °C.[18,19] The control sample comprised pristine VO_2 nanoislands of 40 nm nominal height and lateral dimensions ranging from 50 to 200 nm; the other sample was coated with 5 nm thick gold by electron-beam evaporation, using a quartz crystal microbalance to monitor the thickness. The resulting VO_2/Au-nanomesh is shown in Figure 1a,b.

Below T_c ~ 68 °C, VO_2 is an insulator with monoclinic (M1) structure, while above T_c it is metallic with a rutile (R) structure,[20] accompanied by drastic changes in its near-IR dielectric properties.[19] We compare the switching properties of the pristine and hybrid nanomaterial through broadband transmission hysteresis measurements in which white light from a 3000 K tungsten lamp is focused onto the sample using a 5×, 0.12 NA microscope objective onto the sample and collecting the transmitted light via a 5×, 0.20 NA microscope objective. An InGaAs photodiode placed at the back focal plane of the objective was used to collect the transmitted light while the sample was thermally modulated by a Peltier cooler. The temperature was monitored in situ by a K-type surface-

dx.doi.org/10.1021/nl4044828 | Nano Lett. 2014, 14, 1127−1133

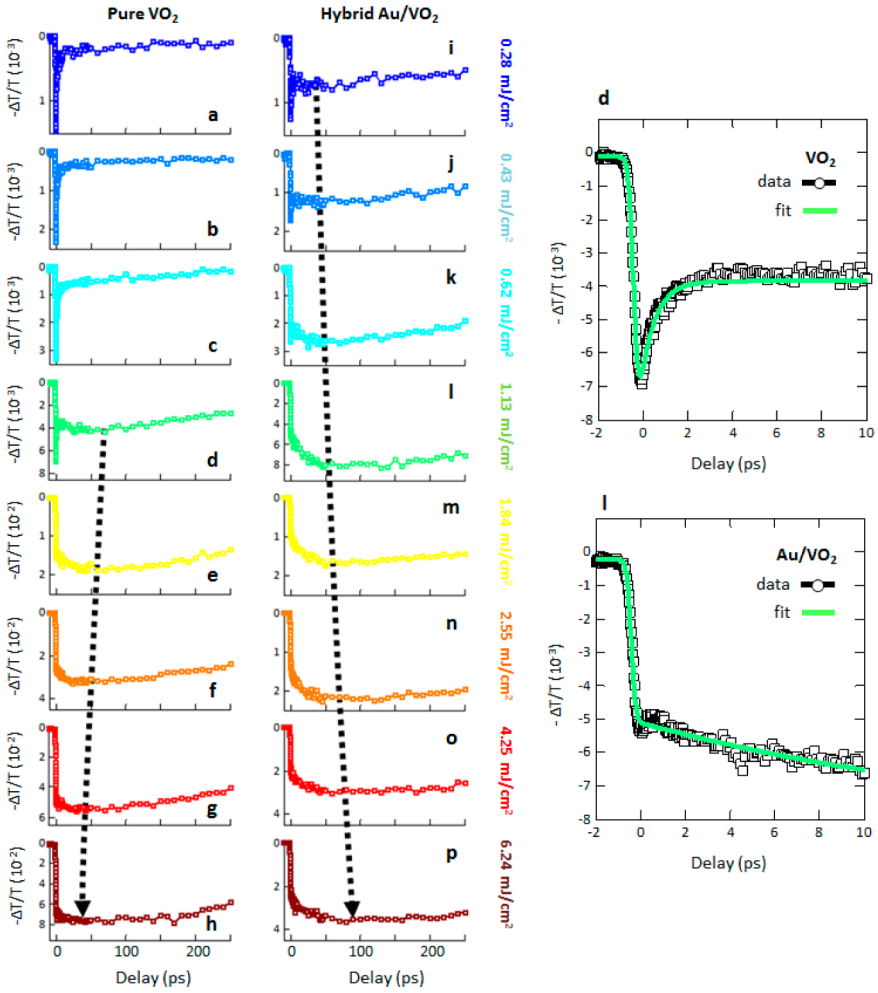

Figure 2. Ultrafast optical measurements. Ultrafast differential transmission data taken at 300 K over a range of 250 ps in pump−probe delay at all pump fluences for pristine VO_2 (a−h) and hybrid Au/VO_2 nanomaterial (i−p). Ultrafast responses for an exciting pump fluence of 1.13 mJ/cm^2 for pristine VO_2 (d) and hybrid Au/VO_2 nanomaterial (l) during the first 10 ps. The open squares are experimental data while the green lines are fits to the data. In (l), complete electronic and structural transformation has already been achieved for the hybrid nanomaterial. The measured rise times for the pristine VO_2 and hybrid nanomaterial samples are 264 ± 28 and 289 ± 31 fs, respectively, comparable within experimental variations. The dotted lines are guides to the eye depicting the approximate point of maximum metallicity. This slower dynamics is discussed in the Supporting Information.

mounted thermocouple. By comparing the critical insulator-to-metal switching temperature (T_c) of the two samples (Figure 1c) we see they behave similarly in the thermal equilibrium regime. Compared to the sharp 1−3 K hysteresis of bulk single-crystal, nanoscale VO_2 exhibits an enhanced hysteresis width because of intrinsic size effects.[21] In the present case, the integrated white-light transmission hysteresis curves exhibit switching temperatures of ∼ 68.1 and 68.7 °C for pristine VO_2 and hybrid Au/VO_2 nanoislands, respectively. The minimal variation in both the phase-transition temperature (T_c ∼ 68 °C) and amplitude of the transmission change (∼ 12%) between the two samples ascertain that the annealing conditions were optimal, that is no conversion to other oxidized phases resulted. This is consistent with earlier experiments that produced switching VO_2 nanoparticles.[18,19,22] More important for our purpose here, deposition of the Au-nanomesh on the PCM does not substantially alter the equilibrium switching properties of either the electronic or structural transitions.

This result is in sharp contrast to a recent study where VO_2 was doped by Au nanoparticles; Au doping drastically modified the thermal character of the VO_2 PT.[23] However, here we observe a constant T_c even when Au coats these smaller nanoscale volumes of VO_2 nanoislands, and even when greater contact electrification effects would, in principle, be noticeable due to strong dependence on effective contact area.[24] Extinction measurements were also acquired by replacing the photodiode with a spectrometer in this quasi-confocal geometry. Spectroscopic measurements (Figure 1d) exhibit the characteristic properties of VO_2, displaying a sharp but static feature at about 390 nm corresponding to the O 2p→V 3d absorption peak and the appearance of a dipolar near-IR response in the VO_2 nanoislands when metallized (darker purple).[19] When normalized to the pristine VO_2 nanoislands, the Au-nanomesh spectra display a plasmonic response centered at 800 nm, near the 790 nm pump wavelength. The resonance of the Au-nanomesh is broadened due to the large size distribution of the underlying VO_2 nanoislands and blue shifts by about 3 nm when VO_2 undergoes its characteristic PT (Figure 1e).[25]

To demonstrate the ultrafast nonequilibrium optical response of the hybrid material, we now compare systematically the differential transmission of both samples in a non-degenerate pump−probe scheme as a function of laser fluence (Figure 2, at 300 K). A 60 fs, 790 nm (1.57 eV) pump pulse

dx.doi.org/10.1021/nl4044828 | Nano Lett. 2014, 14, 1127−1133

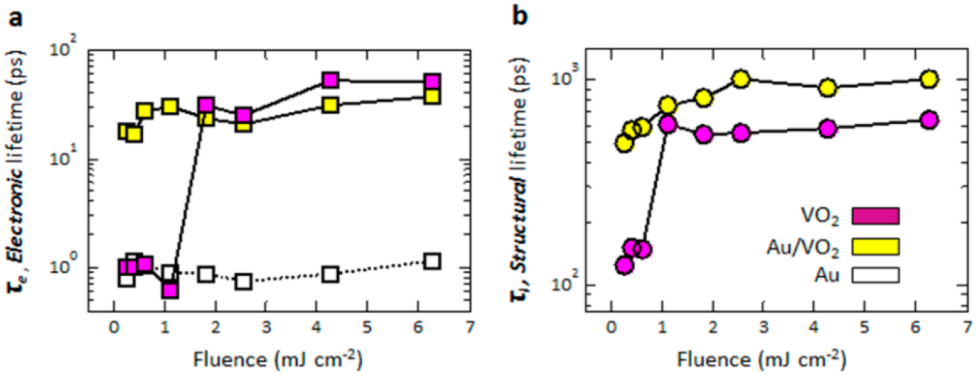

Figure 3. Electronic and structural lifetimes. (a) Electronic decay lifetimes for the Au (empty squares), pristine VO_2 (purple filled squares), and Au/VO_2 nanomaterial (yellow filled squares). Note (i) the electronic lifetime for the Au has a relatively constant value of ~1 ps and (ii) the pristine VO_2 has a switching threshold at about 1.2 mJ/cm^2. (b) Structural lifetimes for VO_2 with (yellow filled circles) and without (purple filled circles) Au-nanomesh. In both (a) and (b), the electronic and structural lifetimes of the Au/VO_2 nanomaterial are already higher than those of the pristine VO_2. In this case, no threshold at the lowest fluences is found, suggesting an already switched state.

above the 0.67 eV VO_2 band gap[26] excites a 67 μm diameter spot on the samples at an angle of 12° with respect to the probe, delayed in time by a translation stage. The probe, generated by optical parametric amplification and incident normal to the sample with a pulse duration of ~40 fs, was tuned to 3100 nm (0.4 eV) to maximize dielectric contrast between the "on" (metallic) and "off" (insulating) states. This enabled detection of only a few hundred μm^3 of PCM-VO_2. At a laser repetition-frequency of 100 kHz, the VO_2 nanoislands recovered to their insulating phase between pulses, confirmed by the negligible background transmission signal at negative time delays.

For the pristine VO_2 nanoislands, pump fluences below threshold result in a large, fast transient transmission that decays rapidly to its original value (Figure 2a–c). This fast-decaying signal resembling a typical semiconductor response is associated with the interaction of the laser field with the electronic system and is characterized by τ_e, the electronic lifetime component of VO_2.[8] However, at a pump fluence of 1.13 mJ/cm^2 (Figure 2d), two ultrafast components emerge, namely a fast electronic response at ~0 fs due to the insulator-to-metal transition accompanied by a gradual, slower response decrease in transmission that reaches a second minimum at about 75 ps, signifying the initial structural transformation of the VO_2 nanoislands, and characterized by a lattice relaxation time, τ_l. This fluence threshold corresponds to one photon interacting with about 70 unit cells and agrees with previous experimental findings when one accounts for the VO_2 filling fraction in our material (see Supporting Information). This minimum in differential transmission is associated with the slower structural dynamics of the monoclinic-to-rutile transition. This signature occurs earlier with increasing fluence and with intensities that create electron densities of order 10^{20}–10^{21} electrons/cm^3 in VO_2, similar to carrier densities in the VO_2 metallic state at thermal equilibrium. Above this threshold, an almost instantaneous transformation to a metallic phase with a characteristic steplike response occurs, corresponding to the rutile (R) structural phase, as described by Cavalleri et al. in ultrafast X-ray studies.[27]

At the lowest pump fluence where only traces of structural PT in the hybrid Au/VO_2 nanoislands are observed (0.28 mJ/cm^2, Figures 2i, 3a,b), each electron created by the Au-nanomesh interacts with about 160 ± 20 unit cells, corresponding to electron densities of roughly 5×10^{19} cm^{-3} in VO_2 (see Supporting Information). Simultaneously, at this lowest fluence, direct photon interactions with the VO_2 lattice create about one electron–hole pair for 400 unit cells. Because the concentration of electron–hole pairs is clearly not sufficient to trigger the structural phase transition in VO_2 (Figure 2a), the injected electrons augment this effect and consequently assist in switching VO_2 even with laser fluences that are below the switching threshold for pristine VO_2 (Figure 2d, 1.13 mJ/cm^2). Although another possible mechanism could be a local electromagnetic field enhancement near the VO_2 due to the plasmonic Au-nanomesh, the modification of carrier density via a Poole-Frenkel effect would instead cause a slow phase transition, driven thermally by electron–lattice coupling and with a picosecond rise time, as demonstrated by Liu et al.[28] Moreover, strong electromagnetic field enhancement derived from split-ring resonators did not affect the intrinsic properties of VO_2 phase transition even at the nanoscale when similar steady-state experiments were carried out.[14] Therefore, in the present case hot-electron injection from the plasmonic Au-nanomesh is the mechanism that activates the subpicosecond PT of VO_2, adding to the incubation effect arising from electron–hole pair generation (Figure 4).

Density functional theory can provide insights into the mechanism by which the injected electrons modify the dynamics of the phase transition. The mechanism responsible for optically induced PT solely in VO_2 has already been the subject of much discussion in the context of an ongoing debate about whether strong electron correlations dominate the response of electrons in VO_2, or whether contrariwise conventional single-particle energy-band formalism, as exemplified in density functional theory (DFT), is sufficient; this debate has been reopened and sharpened with the advent of newer hybrid functionals for the exchange-correlation function.[32] It has been suggested that photogenerated carriers above a critical density screen out the intrasite Coulomb repulsion, leading to the melting of the Mott insulating state.[33] Alternatively, it has been proposed that electron–hole excitations destabilize the V–V dimers, generating excess phonons in the 6 THz band and inducing the phase transition.[31,34,35] Here we used DFT calculations to explore the mechanisms of the optically induced PT and the role of the injected electrons in which the Hubbard U in the GGA+U method is adjusted to provide a satisfactory description of both

dx.doi.org/10.1021/nl4044828 | Nano Lett. 2014, 14, 1127–1133

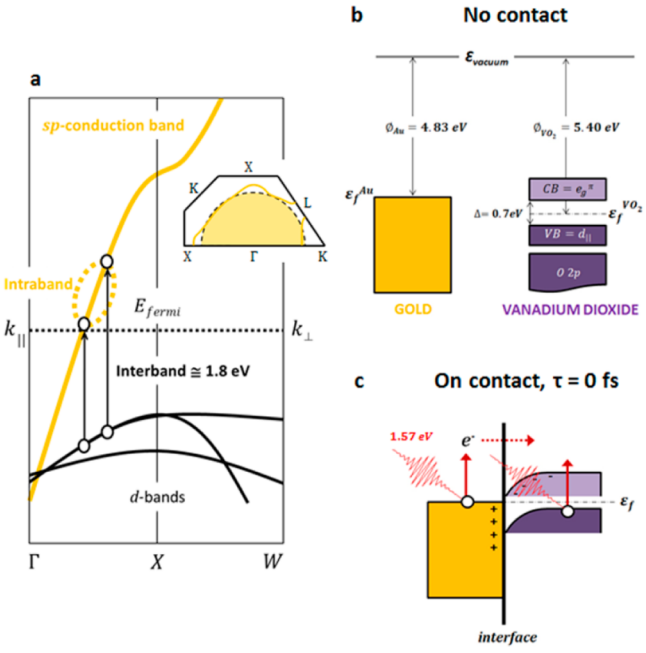

Figure 4. Mechanism of ultrafast switching in hybrid Au/VO_2 nanomaterial. (a) Band structure of gold near the Fermi surface for the lowest possible interband transition; this structure shows that hole injection from *d*-bands is not possible by excitation with a 790 nm (1.57 eV) pump pulse.[29] (b) Energy band diagram of Au and VO_2 before contact with respective work functions adapted from refs 23, 30, and 31. (c) Schematics after contact at $\tau = 0$ ps, when the pump pulse (50 fs, 1.57 eV) both creates hot electrons in Au via intraband transition and excites electrons from the $d_{||}$ valence band to the e_g^{π} conduction band. The hot electrons injected across the interface couple to the cold VO_2 lattice within the first picosecond to overcome the switching threshold and thereby trigger the structural phase transformation concurrently. Following excitation ($\tau > 2$ ps), an ohmic contact is formed when VO_2 transforms from an insulator to a metal.

the insulating and metallic phases of VO_2 (see Supporting Information).

First, we vary the number of electron–hole pairs in a VO_2 supercell comprising 27 monoclinic M1 unit cells by manually placing electrons in the conduction bands and holes in the valence bands, constraining band occupancies accordingly and computing the corresponding phonon spectra. The results are shown in Figure 5. Comparing panels a–c in Figure 5, we see that presence of a single e–h pair per supercell shows softening of the 6 THz mode at the Γ point; introduction of a second e–h pair softens the mode further (see Supporting Information) while exciting four e–h pairs leads to negative frequencies (Figure 5c), which amounts to a destabilization of the VO_2 system leading to the PT. The critical e–h concentration is about 10^{21} cm^{-3}.

Because the presence of holes is known to cause structural relaxation of the V–V dimers[36] we also studied the mechanism of phase transition in purely hole-doped VO_2 by removing electrons from the valence band maximum (VBM). We once again found the 6 THz phonon to soften selectively, reaching negative frequencies at a concentration similar to that for the e–h pair creation (see Supporting Information). Close inspection of the induced electron-density difference (Figure 6) shows that the removed electrons mainly occupied the d_{xy} orbitals of V atoms, the orbitals responsible for the V–V dimer binding.[30] Just as when electron–hole pairs are excited, a similar concentration of holes is required for the 6 THz phonon to reach negative frequencies, confirming that holes play a major role in this ultrafast phase transformation.

We subsequently performed calculations to simulate the injection process, corresponding to the experimental data reported above (Figure 2i–p). These calculations are based on periodically repeated supercells so that the addition of electrons is automatically compensated by a uniform positive background (see Supporting Information for further details). In this case, we see that addition of up to 16 electrons per supercell leaves the phonon spectrum of the VO_2 bulk material virtually

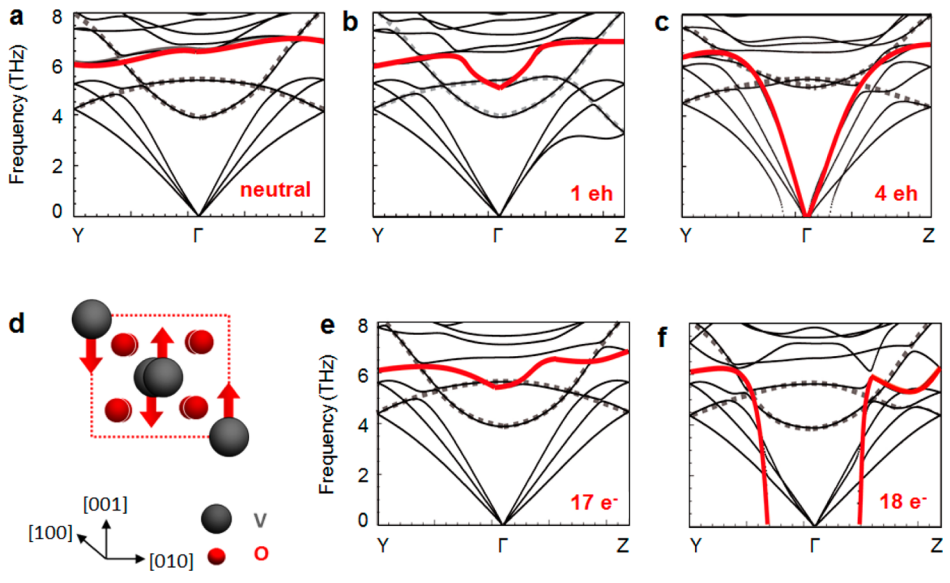

Figure 5. Density functional calculations of phonon spectrum of VO_2. Density functional calculations of the phonon spectra (a) of neutral VO_2 and (b,c) when one and four electrons, respectively, are excited from the valence band maximum to the conduction band minimum. (d) Schematic of the critical phonon mode at 6 THz. Phonon spectra of VO_2 with (e) 17 electrons and (f) 18 electrons injected into the VO_2 supercell. These values correspond to an electron density of about 10^{21} cm^{-3}.

dx.doi.org/10.1021/nl4044828 | *Nano Lett.* 2014, 14, 1127–1133

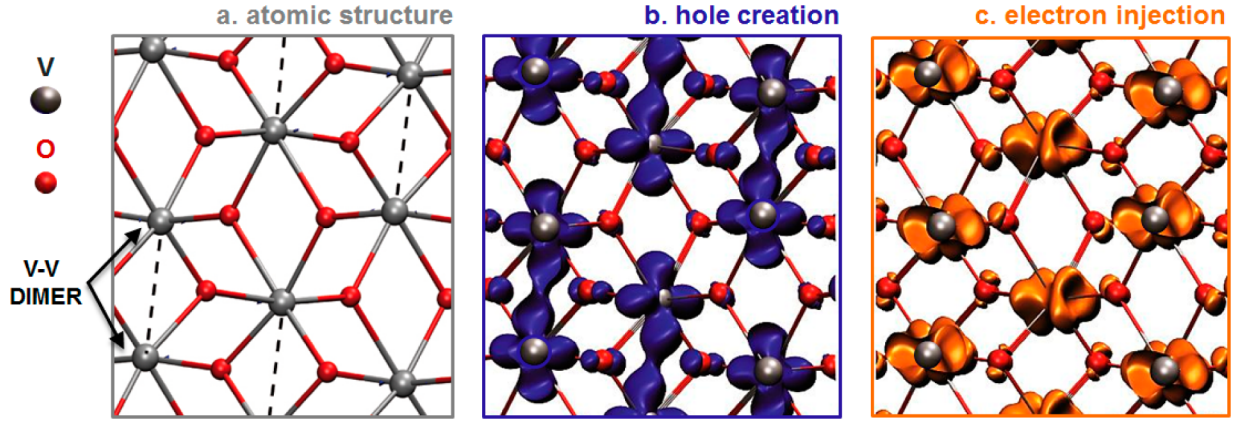

Figure 6. Induced electron-density difference. (a) Atomic structure of VO_2. The dotted lines depict the dimer pairs that connect the vanadium atoms via the $3d_{xy}$ orbitals. (b) Charge density difference resulting from removal of one electron from the valence bands. The isosurface of the hole density is 1.2×10^{-3} e Å^{-3}. (c) Charge density difference between addition of 18 and 16 electrons into the conduction bands. The isosurface of the electron density is 2.4×10^{-3} e Å^{-3}.

unaltered. However, adding a single additional electron to the system (now 17 extra electrons) shows clear sign of the 6 THz softening at the Γ point (highlighted red in Figure 5e) and just one more injected electron (overall 18 extra electrons) results in a catastrophic phonon collapse to a negative frequency (Figure 5f). These excess electrons correspond to an electron density of 10^{21} cm^{-3}, similar to experimental values at saturation level (i.e., when the entire VO_2 volume has switched). While changes to other phonon modes are rather subtle, the collapse of the 6 THz mode is clearly visible. Its atomic motions correspond to the two V atoms forming a V−V dimer vibrating along the [001] direction and tilted from the M1 *a*-axis, as schematically represented in Figure 5d.

Previous experimental work already recognized the role of the 6 THz phonons in triggering the structural phase transition of VO_2,[27,33,34] even suggesting it as an ultrafast marker of the phase transition,[8,37] but its role has been interpreted as the excitation of a critical density of 6 THz phonons.[33] Our calculations show for the first time that the catastrophic collapse of the 6 THz phonon band is a direct consequence of photoexcitation or electron injection, accounting for the experimental finding of an ultrafast phase transition driven by electron injection. Electron injection is less effective than directly removing an electron from the VO_2 orbitals by a factor of about four.

As shown by the calculated spatial maps of induced electron-density difference (Supporting Information Figure S4), the electrons are injected into the spatially extended conduction band of the VO_2, therefore indirectly destabilizing the V−V dimer orbitals. The importance of this orbital contribution to the VO_2 PT has recently been highlighted by Weber et al.[32] The electron injection process discussed here therefore identifies an additional degree of freedom that controls externally the ultrafast properties of PC-VO_2. In the present case, the combined effect of electron injection with electron−hole pair creation in the VO_2, which by itself is not enough to initiate the structural phase transition at the lowest laser fluence (0.28 mJ/cm^2) softens the 6 THz mode up to the point of collapse, marking the onset of the phase transition.

The analysis presented here demonstrates that hot electrons can be harnessed to increase the efficiency with which a phase transformation is triggered on a nonequilibrium, ultrafast time scale. Furthermore, other plasmonic materials with lower work functions together with optimized nanophotocathode architectures can now be designed to meet specific constraints. Because the VO_2 phase transition can also be controlled by hole injection, albeit with lower mobility,[38,39] transistor-like designs that include spectrally selective quantum dots can also be envisioned.[40] Moreover, by examining how plasmonic nanostructures can couple to other transition-metal oxides, for example, by increasing the absorption cross-section, this could result in efficient optically gated electronics,[41] controlling and manipulating materials properties via selective, wavelength-dependent ultrafast creation of nonequilibrium states.

More broadly, using VO_2 as a prototypical PCM, ultrafast electron-injection could modify other phase-transition phenomena via dynamic tuning of the Fermi level, potentially inducing phase transition-like properties in dielectrics as well.[42] In addition, the combination of experiment and theory in this work highlights the essential role played by phonon modes of the VO_2 system in effecting the phase transition. This opens the door to studying the fundamental size limit required for the vibrational modes and phonon density of states to fully develop, thus allowing switching to be realizable in PCMs.[31,43,44] Potentially, one could tailor the emission of coherent acoustic or longitudinal phonon modes to match particular vibrational modes of a PCM to trigger its phase transition.[45]

Ultimately, these studies will enable the design of hybrid nanomaterials with enhanced reconfigurability for realizing all-optical modulators operating at optimizable switching thresholds for the next-generation nanophotonic devices. Such devices would rely on nonequilibrium transient states of these hybrid PT materials that can be manipulated by dynamic charge doping. Hybrid nanomaterials thus have the potential to generate novel ultrafast, nonequilibrium phase-diagrams that reveal emergent dynamical phenomena. However, detailed studies of hybrid nanomaterials dynamics will be necessary to reveal novel physical processes that do not typically occur within one class of material even under equilibrium conditions.

■ ASSOCIATED CONTENT

Supporting Information

Details of the ultrafast measurements, along with details of the computational methods and additional phonon spectra. This material is available free of charge via the Internet at http://pubs.acs.org.

dx.doi.org/10.1021/nl4044828 | *Nano Lett.* 2014, 14, 1127−1133

AUTHOR INFORMATION

Corresponding Authors

*E-mail: (K.A.) krishenappavoo@gmail.com.
*E-mail: (R.F.H.) richard.haglund@vanderbilt.edu.

Author Contributions

K.A. and R.F.H. designed the experiment. K.A., N.F.B., and M.S. conducted the pump−probe experiments. K.A. and J.N. fabricated and characterized the samples. B.W. and S.T.P. performed the DFT calculations. All authors discussed and interpreted the results, and wrote the manuscript.

Notes

The authors declare no competing financial interests.

ACKNOWLEDGMENTS

K.A. and R.F.H. acknowledge support from the Defense Threat-Reduction Agency, DTRA (HDTRA1-10-1-0047). J.N. and R.F.H. acknowledge support from Office of Science, U.S. Department of Energy (DE-FG02-01ER45916. Portions of this work were performed at the Vanderbilt Institute of Nanoscale Science and Engineering, using facilities renovated under NSF (ARI-R2 DMR-0963361). N.F.B. acknowledges support from the U.S. Dept. Education GAANN Fellowship (P200A090143). B.W. and S.T.P. were and were supported in part by DTRA (HDTRA1-10-1-0047), NSF Grant DMR-1207241 and the McMinn Endowment (S.T.P.).This work was performed in part at the Center for Integrated Nanotechnologies, a U.S. Department of Energy, Office of Basic Energy Sciences user facility at Los Alamos National Laboratory (Contract DE-AC52-06NA25396), Sandia National Laboratories (Contract DE-AC04-94AL85000) and by the Laboratory Directed Research and Development Program. The DFT calculations were performed at the DoD Air Force Research Laboratory.

REFERENCES

(1) Zheludev, N. *Nat. Photonics* **2007**, *1*, 551.
(2) Krasavin, A. V.; Zheludev, N. I. *Appl. Phys. Lett.* **2004**, *84*, 1416.
(3) Nasu, K. *Photoinduced Phase Transitions*; World Scientific Publishing Co. Pte. Ltd.: New York, 2004.
(4) Basov, D. N.; Averitt, R. D.; van der Marel, D.; Dressel, M.; Haule, K. *Rev. Mod. Phys.* **2011**, *83*, 471.
(5) Hur, N.; Park, S.; Sharma, P. A.; Ahn, J. S.; Guha, S.; Cheong, S. W. *Nature* **2004**, *429*, 392.
(6) Imada, M.; Fujimori, A.; Tokura, Y. *Rev. Mod. Phys.* **1998**, *70*, 1039.
(7) Millis, A. J.; Shraiman, B. I.; Mueller, R. *Phys. Rev. Lett.* **1996**, *77*, 175.
(8) Wall, S.; Wegkamp, D.; Foglia, L.; Appavoo, K.; Nag, J.; Haglund, R. F., Jr.; Staehler, J.; Wolf, M. *Nat. Commun.* **2012**, *3*, 721.
(9) Sciaini, G.; Harb, M.; Kruglik, S. G.; Payer, T.; Hebeisen, C. T.; Heringdorf, F.; Yamaguchi, M.; Hoegen, M. H. V.; Ernstorfer, R.; Miller, R. J. D. *Nature* **2009**, *458*, 56.
(10) Hada, M.; Zhang, D.; Casandruc, A.; Miller, R. J. D.; Hontani, Y.; Matsuo, J.; Marvel, R. E.; Haglund, R. F., Jr. *Phys. Rev. B* **2012**, *86*, 134101.
(11) Knight, M. W.; Sobhani, H.; Nordlander, P.; Halas, N. J. *Science* **2011**, *332*, 702.
(12) MacDonald, K. F.; Samson, Z. L.; Stockman, M. I.; Zheludev, N. I. *Nat. Photonics* **2009**, *3*, 55.
(13) Lei, D. Y.; Appavoo, K.; Sonnefraud, Y.; Haglund, R. F.; Maier, S. A. *Opt. Lett.* **2010**, *35*, 3988.
(14) Appavoo, K.; Haglund, R. F. *Nano Lett.* **2011**, *11*, 1025.
(15) Ferrara, D. W.; Nag, J.; MacQuarrie, E. R.; Kaye, A. B.; Haglund, R. F. *Nano Lett.* **2013**, *13*, 4169.
(16) Joushaghani, A.; Kruger, B. A.; Paradis, S.; Alain, D.; Stewart Aitchison, J.; Poon, J. K. S. *Appl. Phys. Lett.* **2013**, *102*, 061101.
(17) Kats, M. A.; Blanchard, R.; Genevet, P.; Yang, Z.; Qazilbash, M. M.; Basov, D. N.; Ramanathan, S.; Capasso, F. *Opt. Lett.* **2013**, *38*, 368.
(18) Suh, J. Y.; Lopez, R.; Feldman, L. C.; Haglund, R. F. *J. Appl. Phys.* **2004**, *96*, 1209.
(19) Appavoo, K.; Lei, D. Y.; Sonnefraud, Y.; Wang, B.; Pantelides, S. T.; Maier, S. A.; Haglund, R. F. *Nano Lett.* **2012**, *12*, 780.
(20) Goodenough, J. *J. Solid State Chem.* **1971**, *3*, 490.
(21) Lopez, R.; Feldman, L. C.; Haglund, R. F. *Phys. Rev. Lett.* **2004**, *93*, 177403.
(22) Case, F. C. *J. Vac. Sci. Technol., A* **1987**, *5*, 1762.
(23) Xu, G.; Huang, C. M.; Tazawa, M.; Jin, P.; Chen, D. M.; Miao, L. *Appl. Phys. Lett.* **2008**, *93*, 061911.
(24) Lowell, J.; Roseinnes, A. C. *Adv. Phys.* **1980**, *29*, 947.
(25) Suh, J. Y.; Donev, E. U.; Ferrara, D. W.; Tetz, K. A.; Feldman, L. C.; Haglund, R. F. *J. Opt. A: Pure Appl. Opt.* **2008**, *10*, 055202.
(26) Rini, M.; Hao, Z.; Schoenlein, R. W.; Giannetti, C.; Parmigiani, F.; Fourmaux, S.; Kieffer, J. C.; Fujimori, A.; Onoda, M.; Wall, S.; Cavalleri, A. *Appl. Phys. Lett.* **2008**, *92*, 181904.
(27) Cavalleri, A.; Dekorsy, T.; Chong, H. H. W.; Kieffer, J. C.; Schoenlein, R. W. *Phys. Rev. B* **2004**, *70*, 161120.
(28) Liu, M.; Hwang, H. Y.; Tao, H.; Strikwerda, A. C.; Fan, K.; Keiser, G. R.; Sternbach, A. J.; West, K. G.; Kittiwatanakul, S.; Lu, J.; Wolf, S. A.; Omenetto, F. G.; Zhang, X.; Nelson, K. A.; Averitt, R. D. *Nature* **2012**, *487*, 345.
(29) Beversluis, M. R.; Bouhelier, A.; Novotny, L. *Phys. Rev. B* **2003**, *68*, 115433.
(30) Eyert, V. *Ann. Phys. (Berlin)* **2002**, *11*, 650.
(31) Pashkin, A.; Kubler, C.; Ehrke, H.; Lopez, R.; Halabica, A.; Haglund, R. F.; Huber, R.; Leitenstorfer, A. *Phys. Rev. B* **2011**, *83*, 195120.
(32) Weber, C.; O'Regan, D. D.; Hine, N. D. M.; Payne, M. C.; Kotliar, G.; Littlewood, P. B. *Phys. Rev. Lett.* **2012**, *108*, 256402.
(33) Cocker, T. L.; Titova, L. V.; Fourmaux, S.; Holloway, G.; Bandulet, H. C.; Brassard, D.; Kieffer, J. C.; El Khakani, M. A.; Hegmann, F. A. *Phys. Rev. B* **2012**, *85*, 155120.
(34) Kuebler, C.; Ehrke, H.; Huber, R.; Lopez, R.; Halabica, A.; Haglund, R. F.; Leitenstorfer, A. *Phys. Rev. Lett.* **2007**, *99*, 116401.
(35) van Veenendaal, M. *Phys. Rev. B* **2013**, *87*, 235118.
(36) Cavalleri, A.; Rini, M.; Chong, H. H. W.; Fourmaux, S.; Glover, T. E.; Heimann, P. A.; Kieffer, J. C.; Schoenlein, R. W. *Phys. Rev. Lett.* **2005**, *95*, 067405.
(37) Wall, S.; Foglia, L.; Wegkamp, D.; Appavoo, K.; Nag, J.; Haglund, R. F., Jr.; Stähler, J.; Wolf, M. *Phys. Rev. B* **2013**, *87*, 115126.
(38) Kim, H. T.; Chae, B. G.; Youn, D. H.; Maeng, S. L.; Kim, G.; Kang, K. Y.; Lim, Y. S. *New J. Phys.* **2004**, *6*, 52.
(39) Shah, P. *Ultrafast Spectroscopy of Semiconductors and Semiconductor Nanostructures*; Springer: New York, 1999.
(40) Konstantatos, G.; Badioli, M.; Gaudreau, L.; Osmond, J.; Bernechea, M.; Garcia de Arquer, F. P.; Gatti, F.; Koppens, F. H. L. *Nat. Nanotechnol* **2012**, *7*, 363.
(41) Fang, Z.; Wang, Y.; Liu, Z.; Schlather, A.; Ajayan, P. M.; Koppens, F. H. L.; Nordlander, P.; Halas, N. J. *ACS Nano* **2012**, *6* (11), 10222−10228.
(42) Schiffrin, A.; Paasch-Colberg, T.; Karpowicz, N.; Apalkov, V.; Gerster, D.; Muhlbrandt, S.; Korbman, M.; Reichert, J.; Schultze, M.; Holzner, S.; Barth, J. V.; Kienberger, R.; Ernstorfer, R.; Yakovlev, V. S.; Stockman, M. I.; Krausz, F. *Nature* **2013**, *493*, 70.
(43) Pardo, V.; Pickett, W. E. *Phys. Rev. Lett.* **2009**, *102*, 166803.
(44) Raymand, D.; Jacobsson, T. J.; Hermansson, K.; Edvinsson, T. *J. Phys. Chem. C* **2012**, *116*, 6893.
(45) Subedi, A.; Cavalleri, A.; Georges, A. Theory of nonlinear phonics for coherent light-control of solids. 2013, arXiv:1311.0544 [cond-mat.str-el] (accessed Nov, 2013).